Lattice Boltzmann Model for Dissipative Incompressible MHD

Angus MacNab[1], George Vahala[1], Pavol Pavlo[2], Linda Vahala[3], Min Soe[4]

1. *College of William & Mary, Williamsburg, VA 23187, USA*
2. *Institute of Plasma Physics, Czech Academy, 182 21 Prague, Czech Republic*
3. *Old Dominion University, Norfolk, VA 23529, USA*
4. *Oklahoma Panhandle State University, OK 73939, USA*

In describing transport properties of physical systems one can proceed at various levels of complexity: (a) microscopic, (b) mesoscopic or (c) macroscopic. At the molecular dynamics level there are typically many iterations performed per mean free time. Computationally, this rapidly becomes unmanageable for large number of particles, especially if one is interested in macroscopic properties of the system. The macroscopic level – typically through the appropriate conservation equations – is the straightforward method to solve transport problems. However, macroscopic descriptions face the numerical challenge of solving highly nonlinear pde's. In particular, the accurate representation of the nonlinear convective derivatives $(\mathbf{v}\bullet\nabla)\mathbf{v}$ for the velocity field typically consumes up to 30% of the total CPU in conventional CFD. This nonlinear Riemann problem becomes even more acute in MHD because of the extra nonlinear terms $(\mathbf{B}\bullet\nabla)\mathbf{v}$, $(\mathbf{B}\bullet\nabla)\mathbf{B}$ and $(\mathbf{v}\bullet\nabla)\mathbf{B}$.

The mesoscopic level treats the evolution of the system by a kinetic equation, with the further restriction that collisions are enforced at each time step. The gain in the increase in phase space dimension is the freedom to exploit a linear collision operator (e.g., BGK) in the lattice Boltzmann approach. Moreover, by discretizing the phase space velocity to vectors restricted to a particular lattice, one can minimize the number of degrees of freedom entailed by moving to the mesoscopic level. The resulting mesoscopic description is ideal for massively parallel computers. Indeed, we have seen no saturation, up to the full 512 PE's currently available on the DoE NERSC IBM-SP3 (Fig. 1). In fact, we still see speed-up since the slope is negative. A positive slope would indicate saturation of speed-up with increased number of PE's.

At the mesoscopic lattice Boltzmann level, one typically discretizes

$$\frac{\partial f}{\partial t}+\boldsymbol{\xi}\bullet\nabla f=-\frac{f-f^{eq}}{\tau} \tag{1}$$

on a particular lattice. τ is the rate at which the distribution function f relaxes to f^{eq}. An earlier attempt at a lattice Boltzmann representation for 2D incompressible MHD was by Chen et al. [1]. They utilized a hexagonal lattice together with an auxiliary lattice vector to account for the magnetic field **B**. In essence, there were 36 velocity directions for each spatial node. This model was simplified by Martinez et al. [2] who required only adjacent auxiliary vectors for each lattice direction. This dropped the discrete velocity dimensionality to 13. Here, we will work with an underlying octagonal lattice [3] because of its superior numerical stability properties over the hexagonal or square lattice. The basic octagonal lattice vectors in 2D are thus:

$$\mathbf{e}_n=\left(\cos\frac{2\pi(n-1)}{8}\,,\,\sin\frac{2\pi(n-1)}{8}\right),\quad n=1....8 \tag{2}$$

To each $\mathbf{e}_n$, we introduce auxiliary vectors $\mathbf{e}_\sigma$ orthogonal to $\mathbf{e}_n$: $\mathbf{e}_\sigma = \mathbf{e}_{n\pm2}$ (mod 8). The kinetic velocity space is thus indexed by (n,σ). The discretized kinetic equation is

$$f_n^\sigma(\mathbf{x},t) = \frac{1}{2}\left[f_n^\sigma(\mathbf{x}-\mathbf{e}_n,t-1)+\Omega_n^\sigma(\mathbf{x}-\mathbf{e}_n,t-1)\right]+\frac{1}{2}\left[f_n^\sigma(\mathbf{x}-\mathbf{e}_\sigma,t-1)+\Omega_n^\sigma(\mathbf{x}-\mathbf{e}_\sigma,t-1)\right] \quad (3)$$

with the linear BGK collision operator

$$\Omega_n^\sigma = -\frac{1}{\tau}\left[f_n^\sigma - f_n^{\sigma,eq}\right] \quad (4)$$

Once the lattice is chosen, the only freedom in the lattice Boltzmann method lies in the choice of the relaxation distribution function $f_n^{\sigma,eq}$. $f_n^{\sigma,eq}$ is constrained such that its moments will allow for the recovery of resistive MHD in the Chapman-Enskog long-time large-spatial scales expansions. In particular,

density : $\rho = \sum_{n,\sigma} f_n^{\sigma,eq} + f_0$, where f_0 is the rest particle dist. fn.

momentum : $\rho_0 \mathbf{v} = \sum_{n,\sigma} f_n^{\sigma,eq}\,\mathbf{c}_n^\sigma$, where $\rho_0 = const.$ for incompressible MHD

magnetic field: $\rho_0 \mathbf{B} = \sum_{n,\sigma} f_n^{\sigma,eq}\,\mathbf{d}_n^\sigma$

momentum flux tensor : $\pi_{ij} = \sum_{n,\sigma} f_n^{\sigma,eq}\, c_{n,i}^\sigma\; c_{n,j}^\sigma = \rho c_s^2\delta_{ij} + \rho_0\left(\frac{1}{2}\mathbf{B}^2\delta_{ij} + v_i v_j - B_i B_j\right)$

magnetic flux tensor : $\Lambda_{ij} = \sum_{n,\sigma} f_n^{\sigma,eq} d_{n,i}^\sigma c_{n,j}^\sigma = \rho_0\left(B_i v_j - v_i B_j\right)$ (5)

where we have introduced the vectors $\mathbf{c}_n^\sigma = \frac{1}{2}(\mathbf{e}_n + \mathbf{e}_\sigma)$ and $\mathbf{d}_n^\sigma = \frac{1}{2}(-\mathbf{e}_n + \mathbf{e}_\sigma)$.

These moments are satisfied by the relaxation distribution functions:

$$f_n^{\sigma(eq)} = \frac{1}{4}\rho c_s^2 + \frac{1}{4}\rho_0\ [\ \mathbf{c}_n^\sigma\bullet\mathbf{v} + \mathbf{d}_n^\sigma\bullet\mathbf{B} + 2\left\{(\mathbf{e}_n\bullet\mathbf{v})(\mathbf{e}_\sigma\bullet\mathbf{v}) - (\mathbf{e}_n\bullet\mathbf{B})(\mathbf{e}_\sigma\bullet\mathbf{B})\right\}$$
$$+\left\{(\mathbf{e}_n\bullet\mathbf{v})(\mathbf{e}_\sigma\bullet\mathbf{B}) - (\mathbf{e}_n\bullet\mathbf{B})(\mathbf{e}_\sigma\bullet\mathbf{v}) + \frac{1}{2}\mathbf{v}^2\right\}\ ] \quad (6)$$

and

$$f_0 = \rho\left(1-4c_s^2\right) - 2\rho_0\,\mathbf{v}^2 \quad (7)$$

On performing the Chapman-Enskog expansions, we obtain the resistive MHD equations:

$$\frac{\partial\mathbf{v}}{\partial t} + (\mathbf{v}\bullet\nabla)\mathbf{v} = \nabla\left(P + \frac{\mathbf{B}^2}{2}\right) + (\mathbf{B}\bullet\nabla)\mathbf{B} + \nu\nabla^2\mathbf{v} + O(\nabla\bullet\mathbf{v}, \nabla\bullet\mathbf{B}, ...)$$
$$\frac{\partial\mathbf{B}}{\partial t} + (\mathbf{v}\bullet\nabla)\mathbf{B} = (\mathbf{B}\bullet\nabla)\mathbf{v} + \mu\nabla^2\mathbf{B} + O(\nabla\bullet\mathbf{v}, \nabla\bullet\mathbf{B}, ...) \quad (8)$$

where the error terms include the effects of $\nabla\bullet\mathbf{v}\neq0$, $\nabla\bullet\mathbf{B}=0$ not being explicitly enforced, as well as higher order nonlinear terms.

A major question arises about the MHD constraint $\nabla\bullet\mathbf{B}=0$ [4], especially in multidimensional simulations. The theorists demand $\nabla\bullet\mathbf{B}$ = 0 exactly, and rely on the introduction of the vector potential $\mathbf{A}$, with $\mathbf{B}=\nabla\times\mathbf{A}$. Numerical practitioner generally require that $\nabla\bullet\mathbf{B}\to0$ as the grid resolution $\Delta x\to0$ and time step $\Delta t\to0$, since numerical

errors/roundoff will always occur and the introduction of a vector potential increases the order of the resulting equations and thereby increases the numerical errors. Thus, the magnetic topology will be intact with the enforcement of $\nabla \bullet \mathbf{B} = 0$, but the resulting numerical solutions may be more inaccurate.

Martinez et al. have examined the evolution of $\nabla \bullet \mathbf{B}$ in their lattice Boltzmann BGK simulation and concluded that there seems to be a self-adjusting mechanism which reduces $\nabla \bullet \mathbf{B}$ statistically in time. It must be pointed out that for the hexagonal lattice, Martinez et al. [2] compare their lattice Boltzmann BGK simulations (which have more error terms since they do not introduce a constant ρ_0) to those obtained from a spectral code for the sheet pinch plasma. Very good agreement in time snapshots is found between these codes - and the spectral code does enforce $\nabla \bullet \mathbf{B} = 0$.

Here we present some simulation results on a 1024^2 spatial grid for the Orszag-Tang vortex [5] - see Fig. 2 :

at t = 0 : $\mathbf{v} = \left(\sin(y + 0.5), -\sin(x + 1.4)\right)$, $\mathbf{B} = \left(\sin(y + 4.1), -2\sin(2x + 2.3)\right)$

Initially, the current $\mathbf{J} = J\,\hat{\mathbf{z}}$ has 4 X-points, with 2 large vortices. The current profile develops current sheets at these X-points (Fig. 3).

Acknowledgement: Work partially supported by GACR grant #202/00/1216.

References

[1] H. Chen, W. H. Matthaeus and L. W. Klein, Phys. Fluids **31**, 1439 (1988)
[2] D. O. Martinez, S. Chen and W. H. Matthaeus, Phys. Plasmas **1**, 1850 (1994)
[3] P. Pavlo, G. Vahala and L. Vahala, Phys. Rev. Lett. **80**, 3960 (1998)
[4] G. Toth, J. Computat. Phys. **161**, 605 (2000)
[5] D. Biskamp, Phys. Fluids **B5**, 3893 (1993)

Fig. 1. *Timing results obtained for IBM SP-3.*

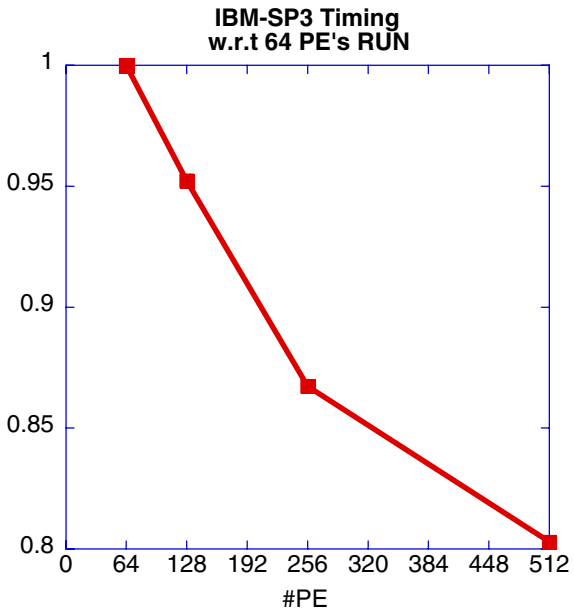

Fig. 2. *Initial current and vorticity profiles for Orszag-Tang 2D vortex.*

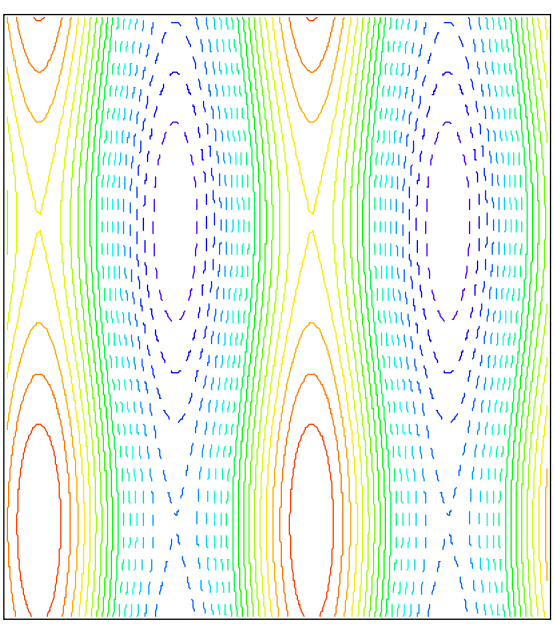

Initial current profile

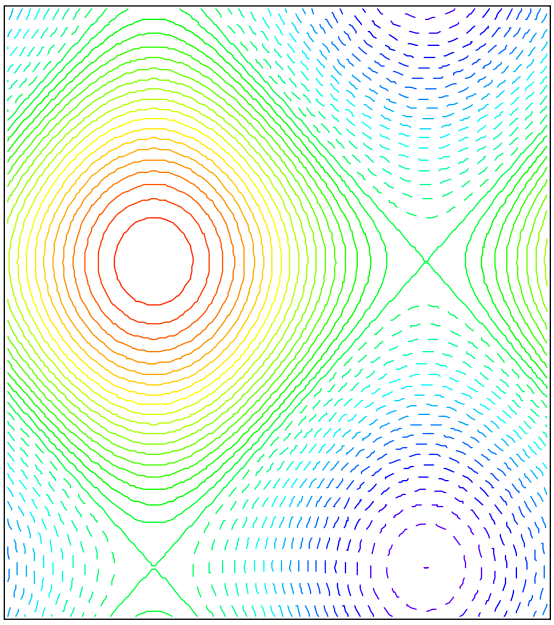

Initial vorticity profile

Fig. 3. *Evolution of the current profile after 100 time steps.*

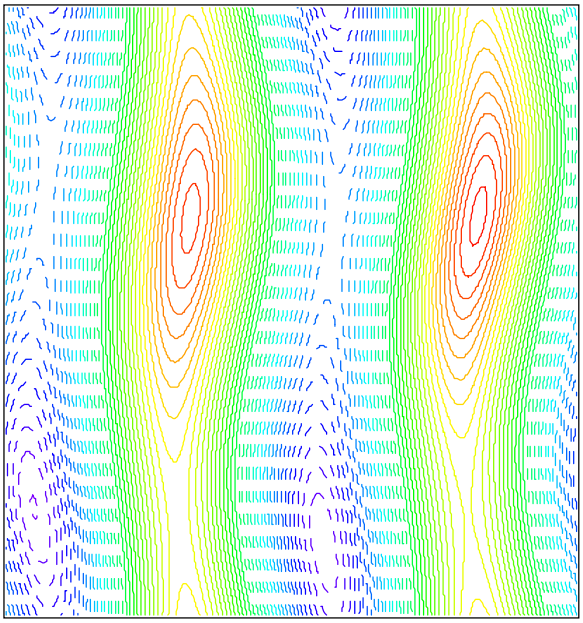

Fig. 4. *Development of current sheets after 1000 time steps.*